Department of Precision and Microsystems Engineering

Parametric study of an elastic singularity-based frequency doubler for concatenation

Luuk Samuels

Report no : 2023.015
Coach : Dr. ir. D. (Davood) Farhadi
Professor : Dr. ir. D. (Davood) Farhadi
Specialisation : Mechatronic System Design (MSD)
Report type : Thesis report
Date : 3-03-2023

TU Delft Delft University of Technology

Preface

The setup of this paper is based on the requirements set by Science for publication. This includes that the materials and methods section is included in the supplemental material. This also means that the paper is focused on results while for any other important details the supplemental material is referenced.

Parametric study of an elastic singularity-based frequency doubler for concatenation

by

L.E.A.M. Samuels

to obtain the degree of Master of Science
at the Delft University of Technology,
to be defended publicly on Friday March 3, 2023 at 14:30

Student number:	4730003	
Project duration:	September 14, 2021 – March 3, 2023	
Thesis committee:	Dr. ir. D. (Davood) Farhadi,	TU Delft, supervisor
	Prof. dr. ir. JL (Just) Herder,	TU Delft, chair
	Dr. ir. S. (Sid) Kumar,	TU Delft

TU Delft

Abstract

The use of elastic frequency multipliers presents the ideal platform to address the coupling between the footprint and range of motion of elastic mechanisms. By transmitting unidirectional into reciprocating motion they efficiently increase the range of motion without a huge compromise in size. In this thesis, an elastic frequency doubler based on an eight-bar mechanism that exploits the displacement around a singularity to double the frequency is presented. Higher frequency multiplications can be achieved by concatenating this mechanism, surpassing previous designs in the literature. To facilitate effective concatenation, criteria for optimization were established and a design study was conducted to determine the optimal geometrical parameters of the mechanism. The utilization of not only the actuation capabilities but simultaneously leveraging the inherently stored strain energy during operation has the potential to serve as the foundation for a novel group of architected materials. The embodiment of both functionalities makes these architected materials highly desirable for control in autonomous robots where, through the exploitation of close synergy and decrease in dissipation, this multifunctionality could increase the efficiency in usage of the usually limited space and available energy.

Introduction

The quest for efficient actuation and energy storage methods has led to the use of elastic mechanisms with programmable outputs. These mechanisms simultaneously embody both functions by harnessing the elastic energy stored in their deformed slender beams. This approach offers some significant benefits such as a monolithic design, more efficient energy utilization, and a close synergy between the functionalities of energy storage and actuation [1]. In this paper, such an elastic mechanism with programmable output will be presented and investigated. The ability to realize a desired mechanical response and the compliance of the mechanism are highly desirable for applications such as the actuation and storage of energy in soft robotics, where these mechanisms could achieve more efficient usage of the already limited space and energy and enable the creation of more capable machines while reducing their mechanical complexity [2, 3, 4, 5, 6, 7]. Or for innovation in mechanical watch design, where the increase in energy and space efficiency due to the monolithic multifunctionality could be exploited [8]. Additionally, the absence of rigid body contact in elastic mechanisms increases their energy efficiency, and life span and decreases the need for maintenance, making them ideal for longevity-promoting low-maintenance environments where energy is often limited such as untethered soft robotics, minimally invasive surgery, the high-tech semiconductor industry, or outer space applications.

It has recently been shown that the fundamental limitation in the range of motion of elastic mechanisms can be overcome through the use of frequency multiplication transmissions [9, 10, 11, 12, 13, 14, 15]. As elastic mechanisms do not allow for infinite continuous rotation, their range of motion (ROM) is fully dependent on the footprint of the mechanism. This limitation is eliminated by instead transmitting unidirectional into reciprocating motion; i.e. frequency multiplication. For mechanisms where the displacement is of equal amplitude a higher frequency is preferred as this increases the ROM.

Recent developments in the field of elastic frequency multipliers are however only limited to the fabrication and testing of a handful of elastic frequency doublers and a single successful concatenation to achieve a frequency quadrupler, while higher frequencies have only been conceptualized. This is attributed to, among other challenges, the difficulty in concatenating these devices to exponentially higher frequencies, due to the desired input-output relations and the limited load capacity of the frequency multiplier building block being unable to handle the increase in actuation stiffness upon concatenation. Additionally, establishing criteria to allow for efficient concatenation has yet to be explored.

The main working principles of elastic frequency multipliers in literature, as described in [16], can be classified into four categories. Firstly, the singularity-based multipliers [14, 15], which involve moving a mechanism around a singularity point to double the frequency. Secondly, the contact-based multipliers [9], that rely on altering the boundary conditions through mid-operation contact with the outside. Thirdly, the tensioned beam multipliers [13], that employ the tensioning and untensioning of beams to change the boundary conditions mid-operation. And lastly, metamaterial-based frequency multipliers [11, 12], where transition waves are guided through the material by either changing the wave-velocity intercellularly or by adding defects to create a reciprocating motion.

Inspired by the recent advancements in elastic frequency multipliers, this study explores a wide design space of parameters for an eight bar based elastic frequency doubler building block that leverages displacement around a singularity to double the frequency, in order to achieve efficient concatenation.

In this paper, we first demonstrate that geometry plays a critical role in determining the qualitative and quantitative behavior of the frequency doubler and that by tuning the geometric variables, the performance can be improved. After this, to facilitate efficient concatenation of the device, we established criteria and performed a wide parameter sweep to identify the optimal geometric parameters. The result of this research has the potential to form the basis of new actuation methods for untethered soft robotics in low-maintenance fields or harsh environments. And is a big step toward embodying both actuation and storage of strain energy into a single monolithic architected material.

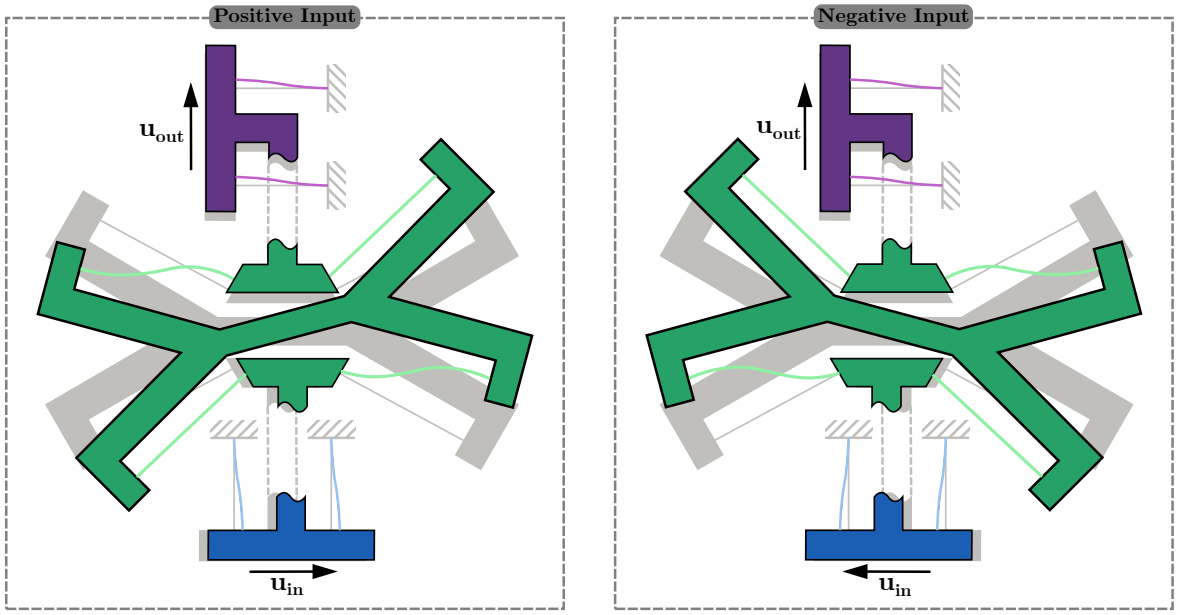

Fig. 1: Deformation of the frequency doubler. Input-output displacement characteristics of the eight-bar mechanism based frequency doubler building block for a positive input displacement **(left)** and a negative input displacement **(right)**.

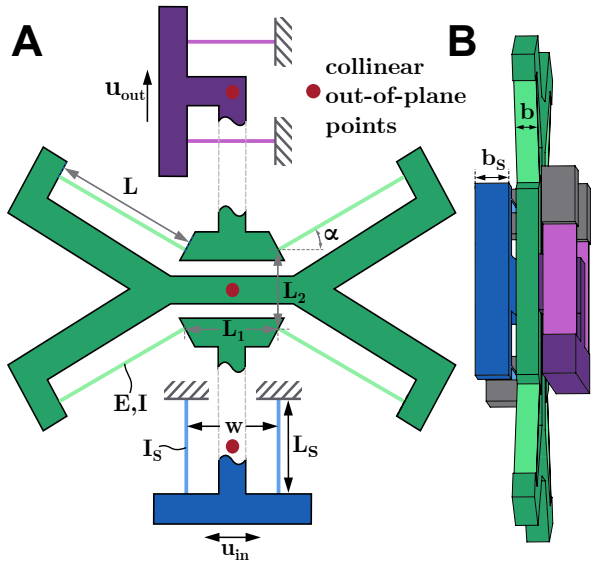

Fig. 2: Important Parameters of the frequency doubler. **(A)** Schematic of the planes of the eight-bar-mechanism based frequency doubler building block. **(B)** Top view showing the mechanisms multiplanarity.

Results & Discussion

Exploiting the singularity

To create a frequency doubling building block that allows for concatenation we explored the behavior of an eight-bar-mechanism based frequency doubler (see Fig. 2). It exploits the movement around a singularity point in the design, making the output shuttle strictly move upwards independent of the direction of the input (as depicted in Fig. 1. The singularity occurs due to the nondeterministic reverse kinematics present for the equilibrium position of the mechanism. This specific design was chosen as it has a good number of tunable variables. The proposed mechanism consists of three parts: the input shuttle (blue) and output shuttle (purple) with thickness (b_s), which function as linear guidances, and the butterfly mechanism (green) with thickness (b). Furthermore, the length between the shuttle's flexures is indicated with (w) and their length with (L_s). To decrease working volume and facilitate easier concatenation the mechanism is made out-of-plane (see Fig. 2 B). This is done in such a way that the center of the three parts are collinear out-of-plane points for a line that is orthogonal to the main plane (see Fig. 2 A). Additionally, this chosen construction also minimizes the resulting moment on the output, by a force on the input, by limiting the moment arm.

To investigate the response of the frequency doubler mechanism finite element analyses (FEA) were conducted for different combinations of the angle, α, normalized length of the butterfly flexures $l = L/u_{in}$ and the normalized horizontal and vertical distance between the butterfly flexures, $l_1 = L_1/u_{in}$ and $l_2 = L_2/u_{in}$ respectively (see Fig. 2), where u_{in} is the maximum displacement of the input shuttle. In the simulations (which were conducted in the enterprise version of 2021R2 Ansys Mechanical APDL) the flexures were modeled as BEAM188 elements based on the Timoshenko beam theory while the rigid bodies were modeled as MPC184 elements assumed as fully rigid due to their relatively large stiffness. Additionally, it uses a linear isotropic material type with Poisson's ratio $\nu = 0.4$, Young's modulus $E = 1700\,\text{MPa}$, yield strength $\sigma_y = 48\,\text{MPa}$, and square cross sections with area moment of inertia $I = 4.86 \times 10^{-13}\,\text{m}^4$ for the butterfly flexures and $I_s = 7.29 \times 10^{-13}\,\text{m}^4$ for the shuttle flexures (See supplementary material for more details on the setup of the simulations).

Influence of design parameters

Having determined the frequency doubling capabilities of the chosen mechanism, we then started investigating if and how changing the earlier defined parameters influences the behavior of the mechanism. This was done by changing some of the variables while looking

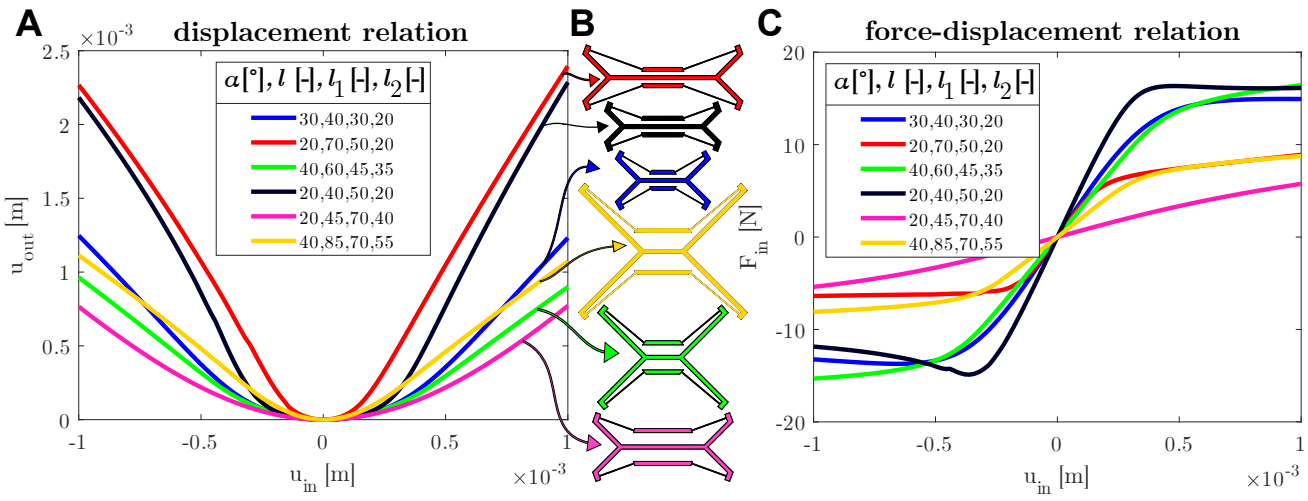

Fig. 3: Geometry and behavior for a handful of designs. (A) Input-output displacement graph showing frequency doubling capabilities and the influence of the geometry. **(B)** Schematics of the designs showing the geometry and size differences. **(C)** Force-displacement graph indicating the influence of geometry on the input stiffness behavior of the designs.

at the displacement transmission (input to output displacement) and the force-displacement relation at the input (see Fig. 3), for changes in behavior. Examining the displacement relation plot (Fig. 3 A), it is evident that changing the parameters within the here specified bounds does not restrict the frequency doubling capabilities that are inherent in each design. However, it can be observed that the geometrical advantage ($G.A.$), which is the relation of the output versus input displacement, nearly quadruples between the designs. And, that each of the designs has a qualitatively different response to the given input. This difference becomes even more evident when observing the force-displacement relation (Fig. 3 C). While one of the designs has an almost linear relation for the whole domain others show only linearity for a smaller domain near the origin. Additionally, it can also be noticed that a transition area is present after which increasing the input displacement causes the stiffness to drop rapidly. For most of the designs, this stiffness stays nonzero and positive, however, some show an almost zero-stiffness behavior while for a single design buckling behavior can even be discerned. The results of our analysis, shown in the plots, demonstrate that modifications in the parameters significantly affect the mechanism's response, and highlight the strong interdependence between the variables.

Establishing criteria for effective concatenation

Having demonstrated that the interdepending geometry of the mechanism has a significant impact on its response, both qualitatively and quantitatively, we proceeded by investigating the desired behavior with concatenation in mind and used this to establish criteria. Three independent criteria were established as the cornerstones for effective concatenation. First of all, the output displacement should be twice that of the input ($G.A. \approx 2$). As in this case, the amplitude of the input and output signal are similar, meaning when concatenated exactly the same motion domain the mechanism is designed for is used. The second criterion is sinusoidality, which is a qualitative analysis of whether a sinusoidal input gives a sinusoidal output with twice the frequency. Sinusoidality was selected instead of the criterion of linearity, exclusively found in literature, for several reasons. One reason is that a linear response from input to output is impossible due to the infinite acceleration occurring near the singularity point. Another reason is that a linear input in the form of a triangular wave consists of a lot of high-frequency vibrations which could cause unwanted resonance in the mechanism or its application. Furthermore, similar to the first reason, a triangular input or output will always be just an approximation due to the impossible infinite acceleration required. In order to achieve a perfect sinusoidal input-output relation the displacement relation has to follow a hyperbolic cosine function (see Supplementary material for more details).

The first two criteria are both fully dependent on the kinematics of the mechanism, however, as the mechanism is essentially a transmission it is also important to look at the influence of a load on the output. This will be done with the third criterion, which is the load capacity of the mechanism and essentially establishes the load it can handle until a certain deviation in kinematics is reached. In this case, the deviation was set to 1%.

In pursuit of identifying the optimal mechanism for the established criteria, the emphasis will be placed on selecting a device that produces a good $G.A.$ as this criterion has the biggest impact on concatenability out of the three. Additionally, to make sure the yield strength of the mechanism is not surpassed during operation a limit on the maximum stress with a safety factor of 1.5 is set (see Supplementary material for more details on the setup of criteria).

Improving the frequency doubler's response

Up to this point, we have demonstrated that the geometry of the design strongly influences the response of the frequency doubler and have determined the necessary criteria for concatenation. Driven by these results, we continued by setting up the design space systematically

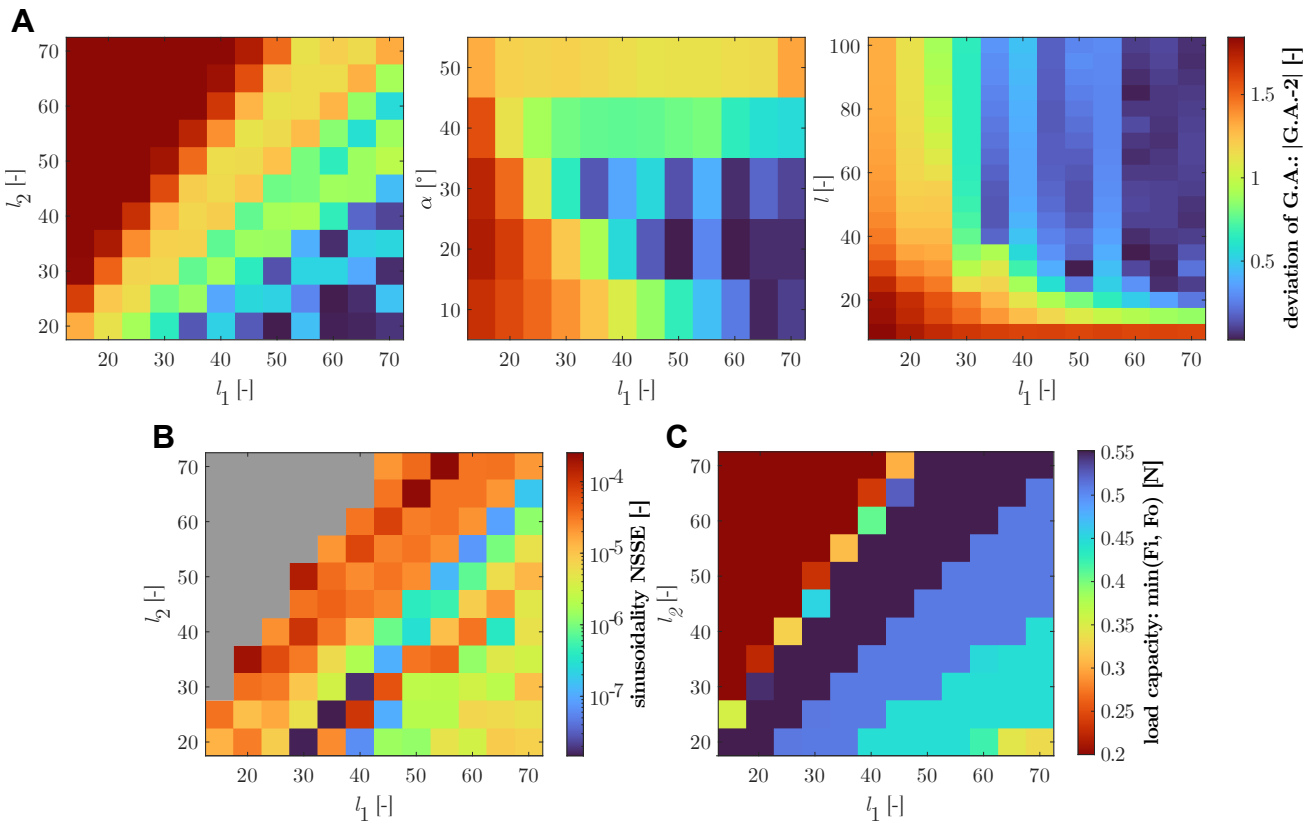

Fig. 4: Mechanical response of the frequency doubler for the preliminary investigation. (A) Evolution of the deviation of the geometrical advantage, $|(G.A.) - 2|$, as a function of the normalized horizontal distance between the butterfly flexures, l_1 and **(left)** the normalized vertical distance between the butterfly flexures, l_2, **(middle)** the angle of the butterfly flexures α, and **(right)** the normalized butterfly flexure length, l. **(B)** Evolution of the sinusoidal normalized sum of square error, Sinusoidal NSSE, as a function of the normalized horizontal distance between the butterfly flexures, l_1, and the normalized vertical distance between the butterfly flexures, l_2. The grey area consists of points where the $G.A. < 0.2$, for which the sinusoidality was not evaluated. **(C)** Evolution of the load capacity, minimum of input force with output constrained and output force with input constrained for 1% of the input displacement, as a function of the normalized horizontal distance between the butterfly flexures, l_1, and the normalized vertical distance between the butterfly flexures, l_2.

with features such as manufacturability, compliance, functionality, and footprint in mind to improve the performance of the frequency doubler. Due to the high-computational cost the resulting wide design space (i.e. $10° \leq \alpha \leq 50°$, $10 \leq l \leq 100$, $15 \leq l_1 \leq 70$ and $20 \leq l_2 \leq 70$) was initially explored with a preliminary investigation of 12,500 design combinations.

In terms of geometrical advantage ($G.A.$) (see Fig. 4 A), it is evident that for smaller values of the horizontal spacing between the flexures (i.e. $l_1 < 35$) and flexure length (i.e. $l < 20$), and larger values of the angle (i.e. $\alpha > 30$) the $G.A.$ does not meet the necessary requirements. Furthermore, an examination of the relationship between the horizontal (l_1) and vertical (l_2) spacing between the flexures reveals that the optimal value of the $G.A.$ is obtained when the horizontal distance is relatively larger (i.e. $l_1 > l_2$). Intuitively this relation is not surprising as a longer input rotation arm compared to the output is required in order to achieve doubling of the input displacement. Similarly, using the same logic, increasing the angle α also decreases the ratio l_1/l_2 needed (see Fig. S15), of which the result can be observed in Fig. 4 A.

Additionally, a clear correlation between the horizontal and vertical spacing is again observable when inspecting the other criteria (Fig. 4 B-C). And, while for load capacity a more equal value for the length is optimal (i.e. $l_1 \approx l_2$) as it reduces the discrepancy between the horizontal input and vertical output load capacity resulting in a higher minimum value, the $G.A.$ and sinusoidality are improved as previously discussed when the horizontal spacing is relatively larger.

Furthermore, analysis of the other parameters for the sinusoidality and load capacity (see Fig. S14), shows that although performance in terms of sinusoidality and load capacity improves with higher values of α, it will ultimately be limited by the worsening of the $G.A.$ for these values. This correlation between the increased load capacity and α can be understood by recognizing that for smaller angles the nearly horizontal flexures do not effectively resist output loads, jeopardizing the load capacity. Meanwhile, for the flexure length (l), which has almost no influence on the deviation of the $G.A.$ as long as $l \geq 20$, a compromise between the sinusoidality that improves with increasing l and the load capacity which worsens with increasing l, as a result of decreased stiffness, will have to be made.

Accompanied by these findings, we were able to narrow down the design space to the more promising areas, to allow us to conduct a more thorough search. In this refined design region (i.e. $10° \leq \alpha \leq 36°$, $30 \leq l \leq 100$, $32 \leq l_1 \leq 74$ and $20 \leq l_2 \leq 50$, with the constraint

$l_2 \leq 0.75l_1 - 2.5$), the primary analysis was carried out coming to a total of 50,000 tested design combinations.

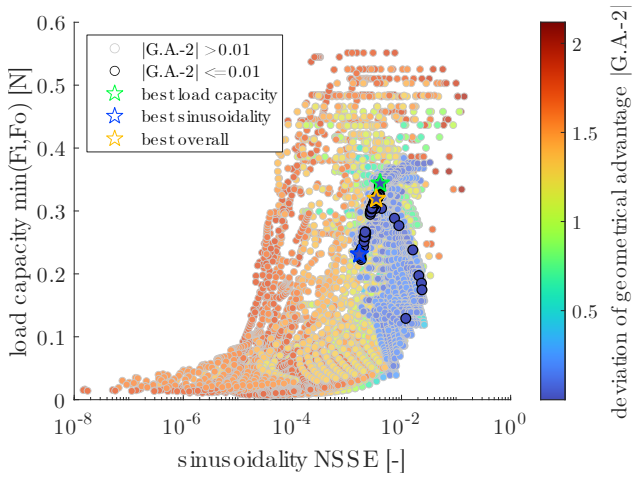

Fig. 5: Best performing designs. Sinusoidal normalized sum of square error, Sinusoidal NSSE, versus load capacity, minimum of input force with output constrained and output force with input constrained for 1% of the input displacement, $min(F_i, F_o)$, versus the deviation of the geometrical advantage, $|(G.A.) - 2|$.

For now, we have explored the complete design space with a preliminary investigation that allowed us to more efficiently explore promising areas with the primary investigation. As this still left room for improvement regarding the resolution between the parameters in the simulations and the criteria, multiple iteration steps were performed with two goals in mind. Firstly to narrow down the search space, allowing for higher resolution searches in narrower spaces. While concurrently tightening the constraints, in order to converge to improved designs (for details see Supplementary material).

The results presented in Fig. 5 demonstrate that achieving the set constraint on the geometrical advantage requires making compromises between sinusoidality and the load capacity. Furthermore, it can be observed that high sinusoidality is only achievable with a low load capacity and $G.A.$. Conversely, designs with optimal load capacity do not perform well in terms of the other criteria. For the set constraint on the $G.A.$ the resulting designs (highlighted with black contours), can only be found in a small area of the full criteria space. Three designs are indicated, first of all, the design with the best load capacity $(\alpha, l, l_1, l_2) = (29.5°, 38.4, 71.8, 41.8)$ for which $G.A. = 2.010$, load capacity $F_c = 0.344\,\mathrm{N}$ and sinusoidality $SSE = 1.7 \times 10^{-3}$. Secondly the design with the best sinusoidality $(\alpha, l, l_1, l_2) = (16.2°, 26.3, 67.8, 23.6)$ for which $G.A. = 1.992$, load capacity $F_c = 0.2313\,\mathrm{N}$ and sinusoidality $SSE = 4.1 \times 10^{-3}$. And lastly, the design that takes the compromise in both to get a better overall behavior $(\alpha, l, l_1, l_2) = (24.8°, 32.7, 71.2, 34.8)$ for which $G.A. = 1.9993$, load capacity $F_c = 0.3195\,\mathrm{N}$ and sinusoidality $SSE = 3.4 \times 10^{-3}$.

Looking at the parameters of these designs again indicates that an increase in the angle of the flexures (α) generally increases the load capacity while worsening the sinusoidality (see also Fig. S18). And furthermore, an increase in the flexure length (l) has a bad influence on the load capacity while improving the sinusoidality (see also Fig. S16-S17).

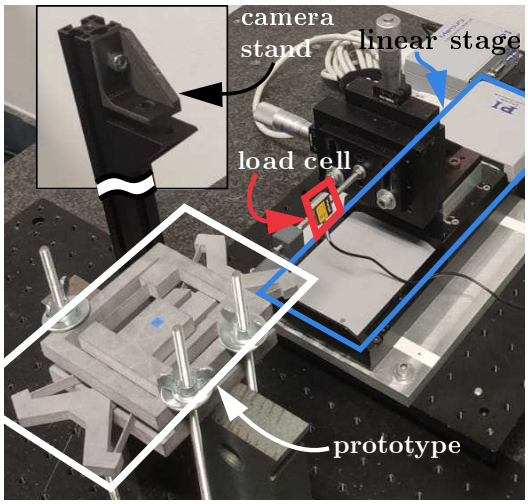

Fig. 6: Experimental setup with prototype. The experimental setup used for validation of the prototype.

Validation

To validate our findings, a prototype, $(\alpha, l, l_1, l_2) = (26.1°, 40.2, 72.6, 37.7)$, of the mechanism was fabricated using Multi Jet Fusion (MJF) and the material Polyamide 12. The prototype was then subjected to tests on the displacement relation and force-displacement by giving an input displacement with a linear stage and measuring the resulting input force with a load cell and the output displacement by tracking a marker (see Fig. 6), of which the results are presented in 7. In order to provide a better representation of the prototype's behavior, the tests were performed over a larger domain than was used in the FE simulations. Subsequently, the simulation was updated to incorporate this modified domain, while simultaneously the flexure thicknesses were modified to more realistically represent the measured thickness inaccuracies of the flexures associated with the manufacturing process. Additionally, as the prototype showed viscoelastic characteristics, such as hysteresis, creep, and stress relaxation the results were averaged over multiple tests (see Supplementary material for more details).

As is evident in Fig. 7 B while comparing the simulation and experimental validation design, especially the behavior of the prototype before the transition area, the area where the stiffness vastly changes, shows a very different force-displacement correlation to the simulation. This is attributed to the fact that in the simulations due to the rigid assumption of the bulk structure, any applied input force is transmitted fully onto the butterfly flexures such that the critical buckling load occurs sooner. And while for the experimental results, it is evident that the stiffness of the structural parts of the prototype can not be assumed as infinite, the critical load, as seen as input force, needed for buckling is still comparable (see also Fig. S12). Additionally, the behavior around and after the transition area, where the behavior of the mechanism is not dictated

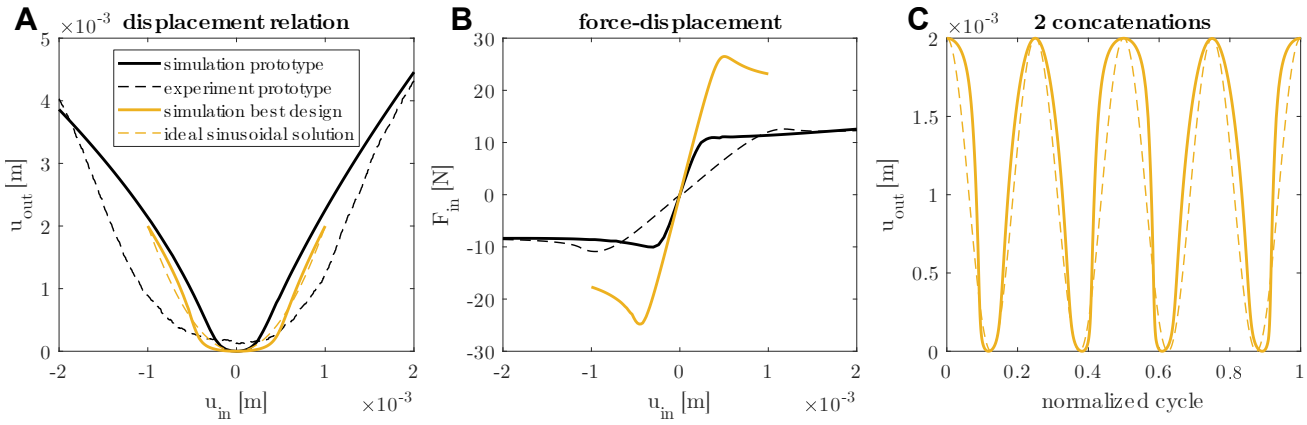

Fig. 7: Validation and the best design (A) Input-output displacement relation for the simulation and experimental result of the prototype $(\alpha, l, l_1, l_2) = (26.1°, 40.2, 72.6, 37.7)$, the best overall design $(\alpha, l, l_1, l_2) = (24.8°, 32.7, 71.2, 34.8)$ and the ideal sinusoidal solution. **(B)** Force-displacement graph. **(C)** Theoretical output displacement versus time for two concatenated frequency doublers, for the ideal sinusoidal input.

by the stiffness of the structure but rather that of the flexures, is in good agreement with the simulation results. Furthermore, inaccuracies in manufacturing and measurements together with the viscoelasticity of the used material also attribute to the lack of correlation between the simulation and experimental result of the prototype (see also Fig. S11 and Fig. S13).

Examining the displacement relation for the manufactured prototype (see Fig. 7 A), it becomes evident that due to the decrease in stiffness before the transition area, the actual prototype has a delayed output displacement increase compared to the simulations (see also Fig. S12). This also leads to almost no output displacement for a relatively large area around the equilibrium point. Furthermore, it can be seen that the experimental result has a more symmetrical response than that shown in the simulations.

Furthermore, analyzing the displacement relation of the best overall design found and comparing it to the ideal sinusoidal solution it can be observed these do not match up perfectly. This is caused by the compromise on the sinusoidality, in order to achieve a better geometrical advantage and load capacity.

Lastly, observing the output displacement after two concatenations, presented in Fig. 7 C, it is evident that the amplitude of the best design is similar to the ideal amplitude, due to the small deviation of the *G.A.* in the best design. Additionally, the variation in frequency over the normalized cycle, due to the added non-sinusoidalities visible in the displacement relation, is clearly observable for the best design.

Further recommended research could be conducted on exploring methods to increase the relative stiffness of the structure compared to the flexures through advanced manufacturing techniques. Furthermore, a deeper investigation into the impact of viscoelasticity on the behavior of the frequency doubler can be undertaken. Finally, research on solving the problem of parity causing highly nonlinear force-displacement behavior when preloading, by statically balancing the frequency doubler building block would be of interest (see also Fig. S5).

Conclusion

In summary, an eight-bar mechanism-based frequency doubler has been explored that utilizes displacement around a singularity to double the input frequency. We have analyzed the influence of the geometry of the frequency doubler on its behavior and have shown how to establish criteria that allow for concatenation. Using these criteria geometrical parameters were identified, allowing for effective concatenation. A prototype was manufactured to validate the displacement and force-displacement relation. The resulting force-displacement indicates a good correlation between the simulation and the prototype's response after the transition area. However, due to the rigid body assumption of the structure in the simulations, the stiffness before this is substantially higher in the simulations. The result of this also shows itself in the displacement relation where due to the delayed buckling of the butterfly flexures the output displacement increase is also delayed. Resulting, in almost no displacement around the equilibrium. Additionally, a theoretical best overall design is identified, indicating the possibilities for efficient concatenation.

When concatenated these mechanisms not only solve the coupling between footprint and range of motion through frequency multiplication but due to their inherent storing of strain energy could embed both functions into a monolithic architected material, which could form the basis for new energy storage and actuation methods highly desirable in the field of soft robotics.

Material & Method

Details on the design can be found in section S1. The method for setting up the simulations is detailed in section S3. Further explanations on the fabrication and experimental setup and validation of the design and prototype are reported in section S4.

Supplementary Materials

Section S1: Design
Section S2: Criteria

References

[1] C. A. Aubin, B. Gorissen, E. Milana, P. R. Buskohl, N. Lazarus, G. A. Slipher, C. Keplinger, J. Bongard, F. Iida, J. A. Lewis, and R. F. Shepherd, "Towards enduring autonomous robots via embodied energy," Nature, vol. 602, no. 7897, pp. 393–402, 2022.

[2] D. Rus and M. T. Tolley, "Design, fabrication and control of soft robots," Nature, vol. 521, no. 7553, pp. 467–475, 2015.

[3] P. Boyraz, G. Runge, and A. Raatz, "An overview of novel actuators for soft robotics," High-Throughput, vol. 7, no. 3, pp. 1–21, 2018.

[4] S. Coyle, C. Majidi, P. LeDuc, and K. J. Hsia, "Bio-inspired soft robotics: Material selection, actuation, and design," Extreme Mechanics Letters, vol. 22, pp. 51–59, 2018.

[5] S. I. Rich, R. J. Wood, and C. Majidi, "Untethered soft robotics," Nature Electronics, vol. 1, no. 2, pp. 102–112, 2018.

[6] T. J. Jones, E. Jambon-Puillet, J. Marthelot, and P. T. Brun, "Bubble casting soft robotics," Nature, vol. 599, no. 7884, pp. 229–233, 2021.

[7] A. Pal, V. Restrepo, D. Goswami, and R. V. Martinez, "Exploiting Mechanical Instabilities in Soft Robotics: Control, Sensing, and Actuation," Advanced Materials, vol. 33, no. 19, pp. 1–18, 2021.

[8] D. Farhadi, J. Herder, G. Semon, and N. Tolou, "Swiss watch featuring dutch precision," vol. Mikroniek:, no. 58(5), pp. 30–34, 2018.

[9] N. D. Mankame and G. K. Ananthasuresh, "A Compliant Transmission Mechanism With Intermittent Contacts for Cycle-Doubling," Journal of Mechanical Design, vol. 129, no. 1, pp. 114–121, jan 2007.

[10] D. N. Haridrabhai, "Towards Micro-mechanical Signal Processors : A Frequency Translator," Indian Institute of Science Bangalore, no. June, 2011.

[11] R. Khajehtourian and D. M. Kochmann, "Soft Adaptive Mechanical Metamaterials," Frontiers in Robotics and AI, vol. 8, no. May, pp. 1–9, 2021.

[12] L. Jin, R. Khajehtourian, J. Mueller, A. Rafsanjani, V. Tournat, K. Bertoldi, and D. M. Kochmann, "Guided transition waves in multistable mechanical metamaterials," Proceedings of the National Academy of Sciences of the United States of America, 2020.

[13] D. Farhadi, J. L. Herder, and N. Tolou, "Frequency doubling in elastic mechanisms using buckling of microflexures," Applied Physics Letters, vol. 115, no. 14, 2019.

[14] D. Farhadi, "Compliant transmission mechanisms," Delft University of Technology, p. 125, 2018.

[15] D. Farhadi, J. L. Herder, G. Semon, and N. Tolou, "A Compliant Micro Frequency Quadrupler Transmission Utilizing Singularity," Journal of Microelectromechanical Systems, 2018.

[16] L. Samuels, "A review on elastic storage mechanisms with a programmable cyclic output," 2022.